Intravital real-time study of tissue response to controlled laser-induced cavitation using 500-ps UV laser pulses focused in murine gut mucosa under online dosimetry and spectrally resolved 2-photon microscopy.

Regina Orzekowsky-Schroeder[1], Antje Klinger[2], Anna Schüth[2], Sebastian Freidank[1], Gereon Hüttmann[1], Andreas Gebert[2], Alfred Vogel[1]

[1]University of Lübeck, Institute of Biomedical Optics, Peter-Monnik-Weg 4, 23562 Lübeck, Germany
[2]University of Lübeck, Institute of Anatomy, Ratzeburger Allee 160, 23538 Lübeck, Germany

ABSTRACT

We present a novel experimental setup to intravitally induce and monitor tissue lesions intravitally at a subcellular level in murine small intestinal mucosa. Using single 355-nm, 500-ps laser pulses coupled to a two-photon microscope, we induced optical breakdown with subsequent cavitation bubble formation in the tissue. Imaging was based on spectrally resolved two-photon excited tissue autofluorescence, while online-dosimetry of the induced microbubbles was done by a cw probe-beam scattering technique. From the scattering signal, the bubble size and dynamics could be deduced on a ns time scale. In turn, this signal could be used to control the damage size. This was important for reproducible production of minute effects in the tissue, despite strong biological variations in tissue response to pulsed laser irradiation.

After producing local UV damage, cells appeared dark, probably due to destruction of mitochondria and loss of NAD(P)H fluorescence. Within 10 min after cell damage, epithelial cells adjacent to the injured area migrated into the wound to cover the denuded area, resulting in extrusion of the damaged cells from the epithelial layer. Using the nuclear acid stain propidium iodide, we could show that UV pulses induced cell membrane damage with subsequent necrosis, rather than apoptosis. For lesions without disruption of the basement membrane, we did not detect migration of immune cells toward the injured area within observation periods of up to 5 hours.

This model will be used in further studies to investigate the intrinsic repair system and immune response to laser-induced lesions of intestinal epithelium in vivo.

Keywords: two-photon microscopy, autofluorescence, in vivo microscopy, UV ns, cavitation, online-dosimetry, tissue repair, wound healing

1 INTRODUCTION / MOTIVATION

Microlesions of intestinal mucosa e.g. due to hard food compounds presumably occur quite often under normal physiological conditions. The intestine is a crucial part of the immune system, because of the huge intestinal mucosal surface which constitutes one of the most important barriers at which the body comes into contact with many pathogens. That raises the question whether those microlesions can significantly influence the immune response of the body. Using laser nanosurgery with UV ns pulses, this physiological situation can be mimicked in vivo under controlled conditions. It has been shown that groups of cells, single cells and subcellular components in the tissue context can be selectively destroyed by optical breakdown and subsequent cavitation bubble formation to study tissue response in vivo [Colombelli04, Colombelli05, Hutson&Ma07]. For the first time, we combine this technique with spectrally resolved two-photon imaging and an optical system for online-dosimetry. With our setup, immune response to lesions of this barrier can be studied in vivo over hours in real time.

2 MATERIALS AND METHODS

2.1 Spectrally resolved two-photon microscopy with laser surgery and online dosimetry

Imaging was done with a two-photon microscope (DermaInspect, Jenlab GmbH) to which a spectral detector with four photomultiplier tubes (PMTs) was added (fig. 1). The dichroics were chosen such that tissue autofluorescence is visible in channels 1-3 (380-450 nm, 450-500 nm, 500-580 nm) while red fluorescent dyes can be detected separately in the fourth channel (580-680 nm).
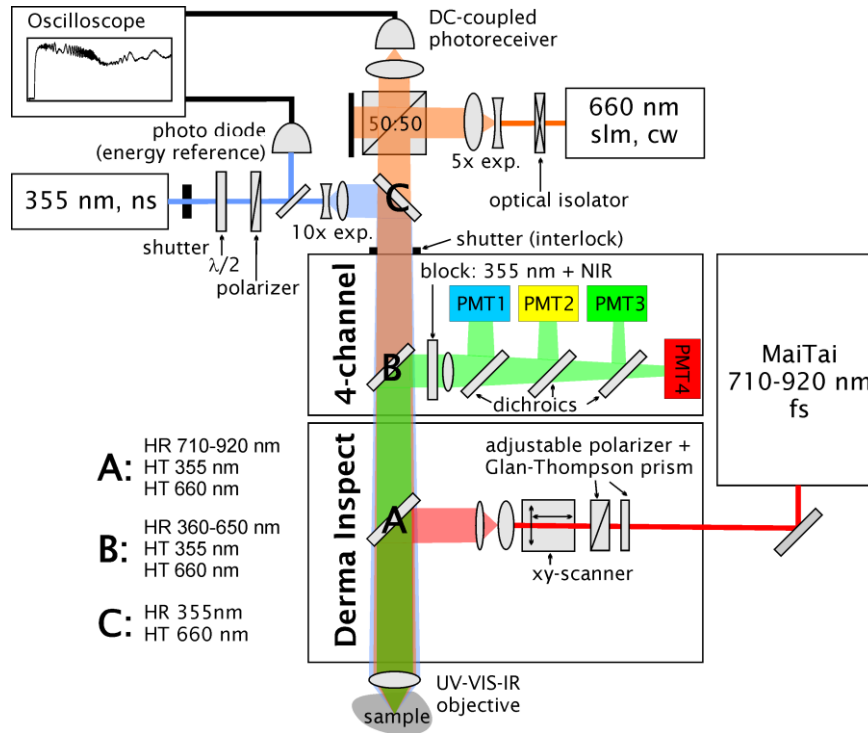
Figure 1: Two-photon microscope (DermaInspect) with spectrally resolved imaging modality (4-channel) and pump-probe setup for UV laser surgery and online dosimetry. PMT=photomultiplier tube, exp. = beam expander, slm = single longitudinal mode, HR = highly reflecting, HT = highly transmitting. For description, see text. (color online)

We coupled a pulsed UV laser at λ=355 nm (3rd harmonic of Nd:YAG λ=1064 nm, τ_{pulse} < 500 ps, teem photonics) to that instrument using the fluorescence pathway. The laser was expanded to fill the back aperture of the objective lens. We used a highly corrected objective lens (40x C-Apochromat/1.2 w UV-VIS-IR, Carl Zeiss GmbH) and adjusted the divergence of the UV laser such that the focus falls within the imaging plane of the two-photon microscope. The maximum pulse energy of the laser system is 30 µJ and could be attenuated by means of a half-wave plate and polarizer. Part of the attenuated beam was deflected by a beam splitter and directed onto a photodiode. The diode's signal was used as energy reference and to trigger the oscilloscope. Single pulses for laser nanosurgery were selected off the 10 Hz pulse train using a mechanical shutter. Aiming for laser surgery was done by two-photon imaging in the apical cytoplasm of epithelial cells in a plane 4 µm below the surface (fig.2 C).

Online-dosimetry of the size of the induced microbubbles was done by a cw probe-beam scattering technique similar to that used in [Vogel08]. The laser energy could this way be adjusted to achieve a preselected bubble size. A 3 mW single longitudinal mode (slm) diode laser (CrystaLaser) at λ=660 nm was coupled into the fluorescence pathway of the two-photon microscope and adjusted collinear and confocal with the UV laser beam. Adapting to the in vivo situation that does not allow for detection in transmission, the signal was collected in a backscattering geometry. Irradiation with

the tightly focussed UV pulses leads to optical breakdown in the tissue with subsequent formation of a cavitation bubble that scatters the cw probe beam. For detection of the backscattered probe light, we used an interferometric setup with a 50:50 beamsplitter and a fast photoreceiver (Femto) (fig. 1). Due to the long coherence length of the slm laser, the backscattered light of the probe beam interferes with the the light that is reflected at the back of the beamsplitter cube, although the path lengths are not identical. From the scattering signal, the bubble size and dynamics can be deduced on a ns time scale as described in sec. 3.1.
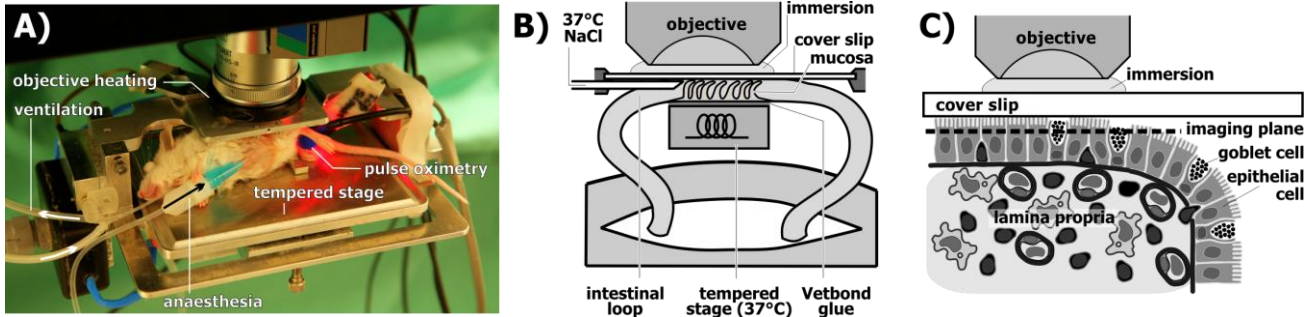
Figure 2: Setup for the investigation of murine intestinal mucosa in vivo **(A)** Anaesthetised balb/c mouse on a homeothermic table. Respiration and oxygen saturation were monitored by pulse oximetry. Physiological temperature (37°C) was maintained by feedback-controlled heating of stage and objective lens. **(B)** During surgical preparation, the abdominal cavity of the anaesthetised mouse was opened and an isolated intestinal loop wa preapred in situ without disturbing the blood supply. The intestine was glued onto a tempered sample stage and sliced lengthwise, so that the mucosa could be carefully pressed to a fixed cover slip. **(C)** Schematic diagram of the intestinal mucosa with examplarily marked imaging and surgical focus plane. (color online)

2.2 Mouse model

We used anaesthetized balb/c mice to access the small intestine in vivo. First a tracheostomy was performed and the mouse was connected to a ventilator (Hugo Sachs Elektronik – Harvard Apparatus GmbH) (fig. 2 A). Then the abdominal cavity was opened and an intestinal loop was gently protruded (fig. 2 B). The loop was glued onto a tempered sample stage and opened legthwise so as to press the luminal side of the tissue slightly against a fixed microscope coverslip. This procedure minimized movement artifacts due to peristalsis. During the experiment, the sample stage was tempered to 37°C and the subject's vital parameters were monitored with a pulse oximeter at the tail vein (MouseOx, Starr Life Sciences) (fig. 2 A).

2.3 Staining protocol

In order to indentify cells with destroyed plasma membrane we used propidium iodide (PI). A drop of PI solution (1 mg/ml in NaCl) was applied in situ and flushed with Ringer solution after 1-10 min. Because PI is membrane impermeant, it enters exclusively cells with defect plasma membranes and intercalates with double-stranded DNA or RNA. When bound to nucleic acids, the fluorescence emission maximum is 617 nm and is detected by PMT 4 (fig. 1).

3 RESULTS AND DISCUSSION

3.1 Bubble dynamics and size

When single UV laser pulses are focussed into living tissue such as murine gut mucosa, minute transient cavitation bubbles are generated by optical breakdown [Hutson&Ma07, Colombelli04, Vogel05]. We observed scattering signals of the probe beam comparable to those arising from cavitation bubbles in water [Vogel08]. The probe beam signals show interference fringes whose frequency decreases while the bubble wall velocity decreases during expansion and increases again during collapse (fig. 3). The frequency is minimal at the turning point of the bubble oscillation when the maximum radius R_{max} is reached. In water, the bubble oscillation time T_{osc} can easily be determined from beginning and first minimum of the scattering signal (ground level). The probe beam signal recovers its original value beacause the water vapor inside the bubble recondenses during the bubble oscillations. The radius of maximum bubble expansion R_{max} can then be calculated from T_{osc} using the Gilmore model which includes surface tension for small bubbles [Gilmore52].
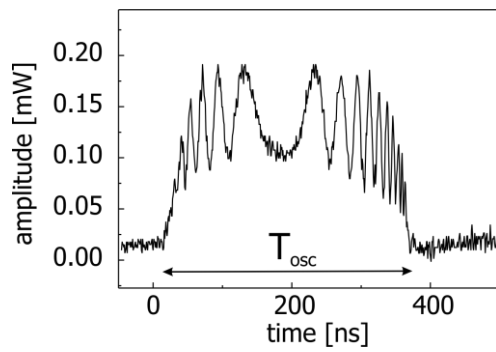
Figure 3: Probe beam signal from scattering at a cavitation bubble in water. The signal shows interference fringes whose frequency decreases while the bubble wall velocity decreases during expansion and increases again during collapse. The oscillation time T_{osc} was determined from beginning and end of the signal to be 356 ns. The signal is highly symmetric during T_{osc}.

In cells or tissue the scattering signals are asymmetric with respect to the point of reversal (maximum bubble expansion), because the collapse is damped due to viscosity and because of plastic deformation of the tissue [Brujan&Vogel06]. Further, the amplitude of the signal does, in most cases, not recover its original value after bubble collapse, which is related to the fact that most likely in the focus non volatile gaseous compounds are formed from dissociated biomolecules, that stay in the focal region for a fairly long time (ms-s). This leads to a residual bubble after collapse which still scatters the probe beam. Therefore, the time $T_{1/2}$ for which the bubble wall velocity is zero, i.e. slowest oscillation in the scattering signal, is used for an estimation of an equivalent oscillation time $T_{osc}=2\ T_{1/2}$ in a compressible liquid. However, for bubbles with very short oscillation times < 200 ns and for some large bubbles, the interference fringes could not be resolved (fig. 5, upper row). For these signals, the oscillation time was determined from beginning and end of the signal (ground level). This case leads to an overestimation of bubble sizes, because the damping viscoelastic properties of the tissue are neglected.

Bubble oscillation times measured in this way are shown in figure 4 as a function of laser pulse energy. The bubble formation threshold is 30 nJ, a value that is about five times lower than the threshold in water. This is due to the presence of endogenous chromophores, such as the reduced form of nicotinamide adenine dinucleotide (NADH), which serve as
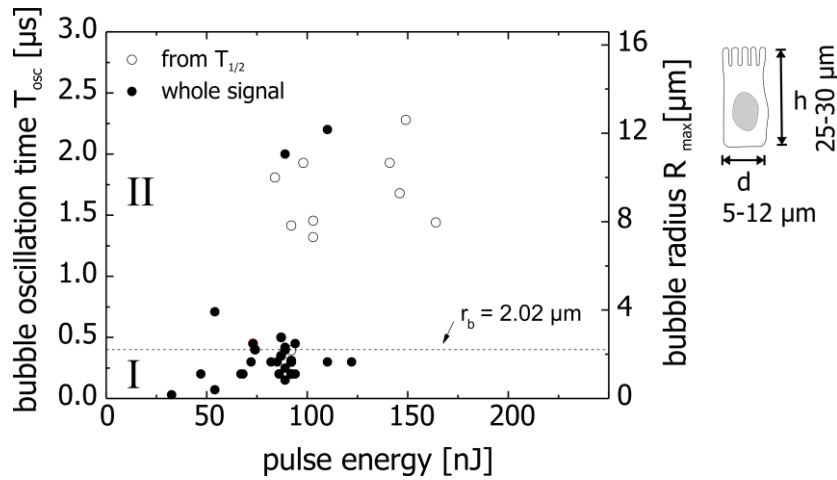
Figure 4: Bubble oscillation times T_{osc} as a function of pulse energy after application of single UV laser pulses (355 nm, 0.5 ns) foucussed with NA 1.2 into intestinal epithelium. The calculated bubble radius R_{max} according to the Gilmore model is plotted on the right scale. Open symbols denote T_{osc} deduced from the turning point of the interference signal. For closed symbols T_{osc} was deduced from the whole signal. Observed signals separate into two classes. **I)** bubbles with T_{osc} < 1 µs, i.e. max. R_{max} < 5 µm (Gilmore, water): visible damage restricted to 1 cell, little or only local autofluorescence reduction, no PI uptake, cell membrane still intact. **II)** bubbles with T_{osc} > 1.5 µs, i.e. R_{max} > 10 µm: at least 5 neighboring cells affected, visible damage spreads within minutes, autofluorescence of affected cells becomes dark, PI uptake, expulsion of damaged cells into the lumen. Dashed line is the calculated oscillation time for a bubble radius of 2.02 µm. This is the size that, for a typical epithelial cell, leads to a membrane enlargement of 4% and would result in membrane rupture [Needham&Nunn90]. For calculation, the shape of an epithelial cell was assumed to be a cylinder with height h and diameter d . The medium was assumed to be water, which leads to an overestimation of bubble sizes.

additional electron sources at low light intensities [Hutson&Ma07]. It can be seen that the signals separate into two classes. Class I contains short bubble oscillation times below 700 ns while class II contains only large bubbles with oscillation times above 1.2 μs. A distinct gap is observed between the bubble sizes in both regimes, but in terms of energy, the regimes show a certain overlap, probably due to local inhomogeneities in linear and nonlinear tissue absorption. Thus, the same pulse energy can induce bubbles of very different size depending on the molecular content in the laser focus.

Cavitation bubbles with a radius of about 2 μm within an epithelial cell of typical dimensions (height 25-30 μm, diameter 5-12 μm) lead to a volume increase such that the cellular plasma membrane would be stretched about 4 %. It has been shown that such lipid bilayer-membranes are destroyed at this strain [Needham90]. It is conceivable that after membrane rupture, bubble expansion suddenly would not be constrained any more to the cellular volume but the bubble could expand freely and thus become larger.

3.2 Immediate tissue effects

Single UV laser pulses of the same energy can lead to very different tissue response. Already at threshold of 30 nJ the effect to the tissue was directly visible in two-photon microscopic images. Target cells showed a strong reduction in autofluorescence (Fig. 5) which was persistent over the observed time span of up to 2 hours.
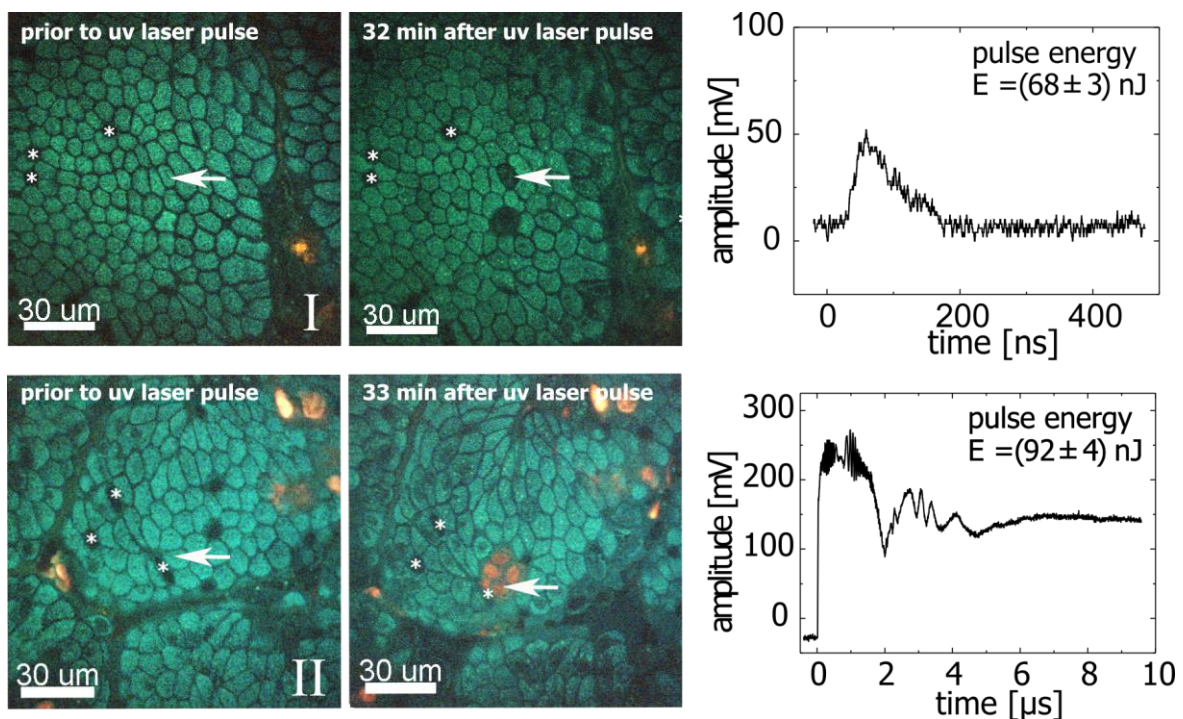
Figure 5: Two-photon excited fluorescence images of intestinal villus epithelium demonstrating two different degrees of damage. In the false color images cellular autofluorescence appears blue-greenish and propidium iodide (PI) is red. Goblet cells appear dark and are marked (*) for orientation. The imaging plane is located 4 μm deep in the apical cytoplasm as shown in fig. 2. **Upper row:** A pulse energy of 68 nJ induces loss of autofluorescence in the target cell (arrow) which turns completely dark within 32 min. after application of the laser pulse. There is no uptake of PI by the target cell within the observed time period. A second cell that was not hit by the UV laser pulse, also loses autofluorescence after a time of increased autofluorescence intensity and is expelled into the lumen. From the scattering signal, an oscillation time t_{osc} = 180 ns and bubble radius r_b = 1.3 μm could be determined. **Lower row:** 92 nJ pulse energy induced damage to a group of 6 adjoining cells. Within 33 min. after the laser pulse these cells loose their autofluorescence and assimilate PI due to severe damage of the cell membrane. PI fluorescence is observed in the nucleus as well as in the cytoplasm of affected cells. Bright PI-stained nuclei appear in the imaging plane indicating a luminal movement of damaged cells. The scattering signal is much stronger and does not return to zero but shows a secondary oscillation. An oscillation time of t_{osc} = 2 $t_{1/2}$ = 1.4 μs and bubble radius r_b = 8.0 μm were determined. (color online)

The scale of damage is strongly correlated to the bubble size deduced from the observed scattering signals. The volume to which the autofluorescence reduction is confined depends on the size of the induced microbubble. For type I bubbles with an oscillation time below 1 µs, i.e. R_{max} below 5 µm, this effect remained confined to the target cell. For type II bubbles with oscillation times > 1.2 µs (radii > 7 µm) the target cell plus 1-3 neighboring cells appeared dark, already directly after the laser pulse. Within minutes after the laser pulse, the damage spread and encompassed up to 10 adjoining cells which also lost their autofluorescence.

The persistent loss of autofluorescence is most likely attributed to the destruction of mitochondrial NADH which is the main endogenous chromophore responsible for two-photon excited autofluorescence [Kierdaszuk96]. NADH shows a maximum in linear absorption at 340 nm and is known to undergo stepwise ionization by a two-photon process at 353 nm [Czochralska&Lindqvist83]. This finding in combination with the scattering signal indicates bubble-induced destruction of mitochondria rather than mere dislocation.

In the experiments with propidium iodide, we observed an uptake of the dye as a result of cell membrane destruction only in cases of type II bubble signals (fig. 5). For the small type I bubbles the cell membrane remained intact. This corresponds well with the calculated bubble radius of 2 microns that is needed for membrane rupture (dashed line in fig. 4). The fact that some of the type I bubble signals fall above that line may be attributed to the systematic overestimation of bubble size. Interestingly, PI entered not only the target cell in which the focus (and thus the bubble) is located but also neighboring cells. Either the mechanical stress due to the cavitation bubble was so large that it directly damaged the adjacent cell membranes or the apoptosis/necrosis of the circumjacent cells was triggerd by signal transduction of the targeted cell. In all cases damage was restricted to the epithelial cell layer and the basement membrane remained intact (fig. 6).
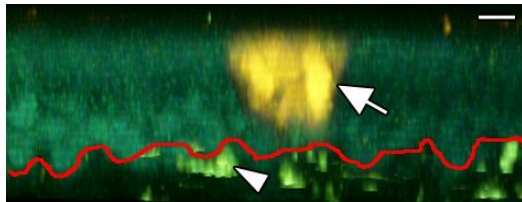
Figure 6: Orthogonal section of intestinal villus epithelium after application of a single UV laser pulse. After 1:08 h, 4 Enterocytes in total have been afflicted and show uptake of propidium iodide (arrow). The basement membrane (red line) shows no disruption and basal cytoplasm of enterocytes is still existent. Scale bar 10 µm. (color online)

3.3 Healing response

In cases in which only single cells were affected by laser surgery, the darkening of the target-cell was the only tissue response to the UV laser pulse observed in vivo within our observation periods of 2 hours (fig. 5). However, for lesions associated with type II bubbles a healing response occured. Damaged necrotic cells were expelled from the epithelial cell layer into the lumen within 10-15 minutes after the laser pulse. This becomes apparent in the sectional images by looking at the bright PI-stained cell nuclei that appear in the imaging plane (figs. 5, 7). At the same time adjacent cells stretch out and move on the basement membrane to cover the denuded area with an approximate speed of 0.4 µm/min (fig. 7). Usually after approximately 30 min. - 1 hour an intact epithelial layer had formed below the necrotic cells, and the villus tip had shortened. At no time resulting gaps in the epithelial layer were observed.

We have repeatedly observed expulsion of single cells (fig. 5) or groups of cells (data not shown) in our in vivo model that was not related to the application of UV laser pulses or any other deliberate external trigger. This is part of the physiological renewal process of epithelial cells in intestinal villi [Potten&Loeffler90]. The fact that this process continues to take place even though the villus has been damaged by UV laser irradiation (fig. 5) indicates that the normal function of the tissue is sustained.

3.4 Immune response

Although villi have primarily a resorptive function, many immune cells such als lymphocytes and antigen presenting cells reside in the lamina propria underneath the villus epithelium or on the basement membrane in between epithelial cells (fig. 1 C). These cells are continuously moving and active. In case of a local epithelial defect, pathogens might have the chance to enter the lamina propria through that tissue lesion and trigger an immune reaction. However, our results do not show any obvious inflammatory reaction, and no directed movement of immune cells towards the defect could be observed. This is probably due to the rapid stretching of adjacent epithelial cells into the region below the injured cells that avoids denudation of the basement membrane and exposure of the immune cells in the lamina propria.
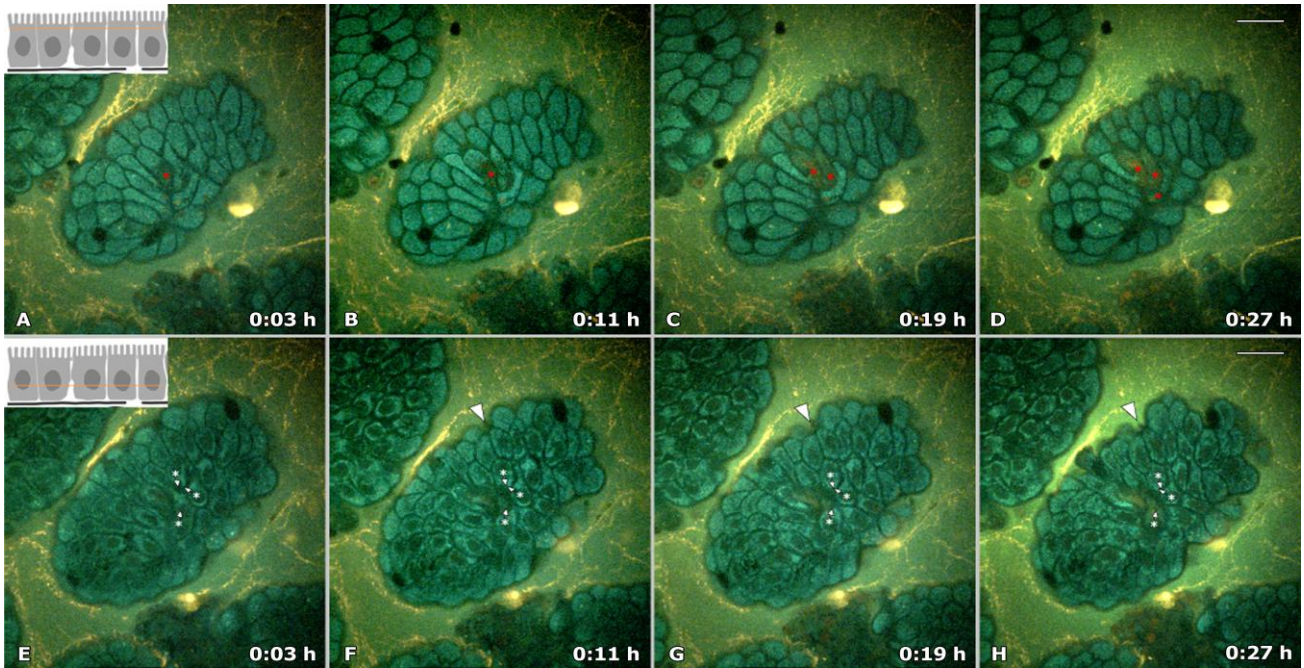
Figure 7: Time series of intestinal villus epithelium after application of a single UV laser pulse and prior luminal addition of propidium iodide. (A-D) Apical cytoplasm and (E-H) basal cytoplasm as shown by inserted focus planes. (A-D) Three minutes after application of UV laser pulse, the target cell (red asterisk) shows a decrease in autofluorescence intensity in two-photon excited fluorescence images (B). Subsequent uptake of red PI fluorescence by the target cell and two additional circumjacent cells (red asterisks) can be observed (B-D; 0:11-0:27 h). (E-H) In the basal focus planes, adjacent epithelial cells (white asterisks) move towards the damaged area with an approximate speed of 0,4 µm/min, to cover the denuded area. Villus contraction can also be observed after UV-laser pulse application (F-H; arrowhead). Scale bar 20µm. (color online)

3.5 Online control of laser tissue effects

Single UV laser pulses of the same energy can lead to very different tissue response (fig. 3), because optical breakdown depends on the applied pulse energy as well as on the distribution of local absorbers. Therefore, laser pulse energy alone cannot be used as a measure for online dosimetry of laser tissue effects. However, the cavitation bubble size is a direct measure for the size of the tissue effect. With our setup, cavitation bubble size can be measured in real time using the probe beam scattering signal. By slowly increasing the laser pulse energy starting below the threshold for cavitation bubble formation, the scattering signal can be used for an automated shut-down of the UV irradiation once the desired size of the effect is reached.

4 SUMMARY AND OUTLOOK

To conclude, we have set up an instrument with which microlesions to the murine small intestine can be induced in a controlled way and can be monitored in vivo over hours. For this we used a pulsed UV-A laser coupled to a two-photon microscope. The size of the lesions can be controlled online via a probe beam technique that makes use of light scattering at the laser-induced cavitation bubbles to adjust the pulse energy of the UV laser.

We observed two regimes of tissue response to single UV pulses which are strongly correlated to the size of the laser-induced microbubbles. Small bubbles with radii < 5 µm at maximum expansion induced damage confined only to the target cell. Autofluorescence was locally reduced due to destruction of mitochondria and the cell membrane remained intact. Bubbles with radii > 7 µm at maximum expansion induced damage to at least 5 neighboring cells associated with autofluorescence reduction, cell membrane rupture and subsequent expulsion of these cells into the lumen. For these lesions adjacent cells stretched out and migrated towards the defect with a speed of 0,4 µm/min. Complete wound healing within 30 min – 1 hour was observed, and no immune reaction occured.

In a next step we will examine whether an immune reaction is triggered if pathogens or foreign particles are present next to a laser-induced lesion in small intestinal mucosa. Further, it will be interesting to study how the body reacts to such lesions in the case of Crohn's disease or other chronic bowel diseases.

To gain a better understanding of cavitation bubble sizes and dynamics in living tissue, the probe beam scattering signals will be compared with ultrashort-time photography.

5 ACKNOWLEDGEMENTS

6 REFERENCES

[Brujan&Vogel06] Brujan, E.-A. and Vogel, A. „Stress wave emission and cavitation bubble dynamics by nanosecond optical breakdown in a tissue phantom", J. Fluid Mech. 558, 281-308 (2006)

[Colombelli04] Colombelli, J., Grill, S.W., Stelzer, E.H.K., „Ultraviolet diffraction limited nanosurgery of live biological tissues", Rev. Sci. Instr., 75, 472-478 (2004)

[Colombelli05] Colombelli, J., Reynaud, E.G., Stelzer, E.H.K., „Subcellular nanosurgery with a pulsed subnanosecond UV-A laser", Med. Laser App., 20, 217-222 (2005)

[Czochralska&Lindqvist83] Czochralska, B. and Lindqvist, L., "Biphotonic one-electron oxidation of NADH on laser excitation at 353 nm", Chem. Phys. Lett. 101, 297-299 (1983)

[Gilmore52] Gilmore, F.R., "The collapse and growth of a spherical bubble in a viscous compressible liquid", Calif. Inst. of Tech. Hydrodynamics Lab. Report No. 26-4 (1952)

[Hutson&Ma07] Hutson, M.S. and Ma, X.,, Plasma and cavitation dynamics during pulsed laser microsurgery in vivo", PRL. 99, 158104 (2007)

[Kierdaszuk96] Kierdaszuk, B. et al., "Fluorescence of reduced nicotinamides using one- and two-photon excitation", Biophys. Chem. 62, 1-13 (1996)

[Needham&Nunn90] Needham, D., Nunn, R.S., „Elastic-deformation and failure of lipid bilayer-membranes containing cholesterol", Biophys. J. 58, 997 (1990)

[Potten&Loeffler90] Potten, C.S. and Loeffler, M. "Stem cells: attributes, cycles, spirals, pitfalls and uncertainties. Lessons for and from the crypt." Development 110, 1001-1020 (1990)

[Vogel05] Vogel, A., Noack, J., Hüttmann, G., and Paltauf, G., "Mechanismas of femtosecond laser nanosurgery of cells and tissues", Appl. Phys. B, 81, 1015-1047 (2005)

[Vogel08] Vogel, A., Linz, N., Freidank, S., and Paltauf, G., „Femtosecond-laser-induced nanocavitation in water: implications for optical breakdown threshold and cell surgery", PRL 100, 038102 (2008)